Inorganic Chemistry

Article

pubs.acs.org/IC

Probing the Electronic Properties of a Trinuclear Molecular Wire Involving Isocyanoferrocene and Iron(II) Phthalocyanine Motifs

Victor N. Nemykin,*[,†] Anatolii A. Purchel,[†] Andrew D. Spaeth,[‡] and Mikhail V. Barybin*[,‡]

[†]Department of Chemistry and Biochemistry, University of Minnesota—Duluth, 1039 University Drive, Duluth, Minnesota 55812, United States

[‡]Department of Chemistry, University of Kansas, 1251 Wescoe Hall Drive, Lawrence, Kansas 66045, United States

Supporting Information

ABSTRACT: A new trinuclear iron(II) complex involving two isocyanoferrocene ligands axially coordinated to iron(II) phthalocyanine, $(FcNC)_2FePc$ [Fc = ferrocenyl; Pc = phthalocyaninato(2−) anion], was isolated and characterized using a variety of spectroscopic methods as well as single-crystal X-ray diffraction. The redox behavior of the above molecular wire was investigated through electrochemical, spectroelectrochemical, and chemical oxidation approaches and compared to that of the bis(*tert*-butylisocyano)iron(II) phthalocyanine reference compound, $(t\text{-BuNC})_2FePc$. For both complexes, the first oxidation involves the phthalocyanine ligand and results in the formation of a red phthalocyanine cation-radical-centered $[(RNC)_2FePc]^+$ species, as evidenced by their UV−vis and electron paramagnetic resonance spectra. Despite the ∼11.5 Å distance between the isocyanoferrocene iron centers, the second and third oxidation potentials for $(FcNC)_2FePc$ are separated by ∼80 mV, which is indicative of a weak long-range metal−metal coupling in this system. Spectroscopic signatures of the mixed-valence $[(FcNC)_2FePc]^{2+}$ dication were obtained using spectroelectrochemical and chemical oxidation approaches. These experimentally assessed characteristics were also correlated with the electronic structure, redox properties, and spectroscopic signatures predicted by density functional theory (DFT) and time-dependent DFT analyses.

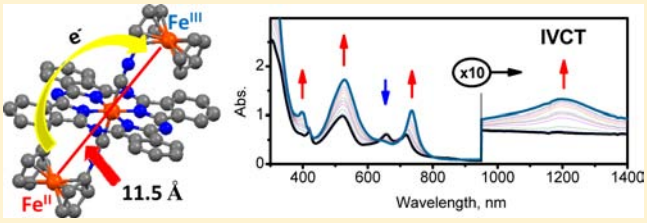

INTRODUCTION

Polynuclear transition-metal-containing organometallic assemblies with tunable electron-transfer, redox, and optical characteristics are attractive as building blocks for molecular electronics and light-harvesting systems.[1] In particular, complexes featuring ferrocenyl groups attached to thermally, chemically, and photochemically stable tetraazaporphyrins,[2] phthalocyanines (Pc's),[3] corroles,[4] and especially porphyrins[5] have been intensively studied during the past several decades. Such organometallic−aromatic macrocycles often exhibit prominent intramolecular metal−metal coupling and have been suggested as new materials for random-access memory devices, molecular wires, optical limiters, redox-switchable fluorescence markers, and active components in electro- and photocatalytic reactions.[6] In most cases, the ferrocenyl substituents are connected to the macrocycle directly or through a variety of linking groups, while reports on porphyrins and their analogues featuring axially coordinated redox-active organometallic units through covalent bonding with the central metal atom in the macrocycle are quite rare.[7]

Capable of functioning as both good σ donors and strong π acceptors,[8] organic isocyanides can form very stable, axially coordinated complexes with iron(II) and ruthenium(II) phthalocyanines.[9] Hanack and co-workers have shown that supramolecular coordination assemblies involving linear diisocyanoarenes and iron(II) phthalocyanines (PcFe) have semiconducting properties.[10] Despite significant efforts aimed at understanding fundamental interactions between isocyanides and porphyrinoids, axial coordination of redox-active organometallic isocyanides[8] and iron(II) or ruthenium(II) porphyrinoids is yet to be considered, although such systems could be prominent candidates for molecular wires. In this article, we introduce the first example of such an axial assembly that features redox-active isocyanoferrocene (FcNC) ligands bound to the PcFe core and discuss its electronic structure and redox properties established using a variety of spectroscopic, electrochemical, and spectroelectrochemical approaches, as well as density functional theory (DFT) and time-dependent DFT (TDDFT) methods. The properties of $(FcNC)_2FePc$ will be compared and contrasted with those of the known "reference" complex $(t\text{-BuNC})_2FePc$.

EXPERIMENTAL SECTION

Materials. All reactions were performed under a dry argon atmosphere with flame-dried glassware. All solvents and reagents were purchased from commercial sources. Toluene was distilled over sodium metal. Dichloromethane (DCM) was distilled over CaH_2. Tetrabutylammonium tetrakis(pentafluorophenyl)borate (TBAF)[11]

Received: May 7, 2013
Published: August 28, 2013

   dx.doi.org/10.1021/ic4011423 | *Inorg. Chem.* 2013, 52, 11004−11012

and isocyanoferrocene (FcNC)[12] were prepared according to literature procedures.

Instrumentation. ^{1}H and ^{13}C NMR spectra were collected at 500 and 125 MHz, respectively, using a Varian Unity INOVA NMR instrument. The ^{1}H and ^{13}C chemical shifts are given in parts per million (ppm) with reference to Me_4Si as an internal standard. All UV−vis data were obtained on a JASCO-720 spectrophotometer at room temperature. An OLIS DCM 17 CD spectropolarimeter with a 1.4 T DeSa magnet was used to obtain all magnetic circular dichroism (MCD) data. Cyclic voltammetry (CV) and differential pulse voltammetry (DPV) measurements were conducted using a CHI-620C electrochemical analyzer utilizing a three-component system consisting of a carbon or platinum working electrode, a platinum wire auxiliary electrode, and a glass-encased nonaqueous silver/silver chloride reference electrode. A 0.05 M solution of TBAF or a 0.1 M solution of tetrabutylammonium perchlorate (TBAP) in DCM was employed as the supporting electrolyte. In all cases, the redox potentials are referenced to the FcH/FcH^+ couple using decamethylferrocene as an internal standard. Spectroelectrochemical data were collected in a 0.15 M solution of TBAF or a 0.3 M solution of TBAP in DCM using a custom-made 0.1 cm cell equipped with a working electrode made of platinum mesh. In order to ensure accurate data collection on closely spaced oxidation processes for $(FcNC)_2FePc$ and account for any potential shift between electro- and spectroelectrochemical cells, the applied potentials were varied in 20 mV increments during the spectroelectrochemical experiments involving the $[(FcNC)_2FePc]^+ \rightarrow [(FcNC)_2FePc]^{2+} \rightarrow [(FcNC)_2FePc]^{3+}$ transformations. IR spectra were recorded in KBr pellets using a Perkin-Elmer Spectrum 100 instrument. All electron paramagnetic resonance (EPR) measurements were carried out with an X-band Bruker EMX Plus spectrometer with a dual-mode cavity operating in perpendicular mode using Oxford Cryostat at 77 K. *Xenon* software (version 1.1.b.44) was employed for EPR spectra acquisition and baseline correction. Elemental analysis was performed by Atlantic Microlab, Inc., in Atlanta, GA. Chemical titration experiments were typically conducted using 1.0×10^{-6}−3×10^{-6} M solutions of Pc complexes and $\sim 1.0 \times 10^{-3}$ M stock solutions of oxidants added in 0.1−0.3 equivalent increments.

Synthetic Work. *Synthesis of $(FcNC)_2FePc$.* A total of 56.8 mg (0.0001 mol) of iron(II) phthalocyanine was added to a solution of 422 mg (0.002 mol) of the FcNC ligand in 15 mL of toluene under an argon atmosphere. The reaction mixture was heated to 80 °C for 4 h and then filtered under argon. The precipitate was washed several times with hot toluene, and the toluene filtrate was reduced in volume to 10 mL. After overnight cooling of the resulting solution at 0 °C, the target $(FcNC)_2FePc$ product was filtered off and washed several times with hot hexanes. The solid was recrystallized from dry DCM/hexanes to form the analytically pure $(FcNC)_2FePc$ complex. Yield: 22 mg (22.2%). ^{1}H NMR (500 MHz, $CDCl_3$): δ 9.39 (m, 8H, α-Pc), 8.01 (m, 8H, β-Pc), 3.20 (s, 4H, β-H's of C_5H_4NC), 3.14 (s, 10H, C_5H_5), 2.66 (s, 4H, α-H's of C_5H_4NC). ^{13}C NMR (125 MHz, $CDCl_3$): δ 147.1 (α-pyrrole), 141.3 (β-pyrrole), 128.0 (α-Pc), 121.1 (β-Pc), 70.0 (C_5H_5), 65.8 (β-C's of C_5H_4NC), 65.4 (α-C's of C_5H_4NC), 45.1 (*ipso*-C of C_5H_4NC). Because of the often[8] broad nature of the ^{13}C NMR signal for the isocyano carbon atom, it was not clearly observed in the spectrum of $(FcNC)_2FePc$. UV−vis [DCM; λ, nm (log ε, M^{-1} cm^{-1})]: 662 (5.08), 634sh, 599 (4.56), 394 (4.34), 321 (4.92). IR (KBr): 2132 [ν(CN)], 3082, 3056, 1643, 1611, 1508, 1421, 1330, 1287, 1164, 1119, 1096, 1076, 777, 753, 729, 483 cm^{-1}. Anal. Calcd for $(FcNC)_2FePc \cdot 1.75CH_2Cl_2$ (found): C, 58.78 (58.44); H, 3.32 (3.88); N, 12.30 (12.72). The presence of a DCM solvent of crystallization was observed in the ^{1}H NMR spectrum of this sample. Selected X-ray crystallographic data: $P2_1/c$ (monoclinic), a = 10.7210(7) Å, b = 25.8739(10) Å, c = 9.5479(4) Å, β = 91.161(6)°, volume = 2648.0(2) Å^3, total reflections collected 17068, independent reflections 6062, R(int) = 0.056, R1 [$I > 2.0\sigma(I)$] = 0.0505, wR2 (all) = 0.0934, GOF = 0.983.

Synthesis of $(t\text{-BuNC})_2FePc$. This known compound was prepared using a slightly modified version of the previously reported[13] synthetic procedure. A total of 113.6 mg (0.0002 mol) of iron(II) phthalocyanine was added to a solution of 5 mL of the *t*-BuNC ligand in 25 mL of toluene under an argon atmosphere. The reaction mixture was heated to 80 °C for 4 h and then filtered under argon. The precipitate was washed several times with hot toluene, and the toluene filtrate was reduced in volume to 15 mL. After overnight cooling of the resulting solution at 0 °C, the target $(t\text{-BuNC})_2FePc$ product was filtered off and washed several times with hot hexanes. The solid was recrystallized from dry DCM/hexanes to form a pure $(t\text{-BuNC})_2FePc$ complex. Yield: 278 mg (63.8%). ^{1}H NMR (500 MHz, $CDCl_3$): δ 9.33 (dd, 8H, α-Pc), 7.98 (dd, 8H, β-Pc), −0.51 (s, 18H, CH_3). UV−vis [DCM; λ, nm (log ε, M^{-1} cm^{-1})]: 659 (5.08), 635sh, 597 (4.58), 395 (4.26), 322 (4.92). IR (KBr): 2146 [ν(CN)], 3058, 2980, 1589, 1508, 1465, 1421, 1371, 1328, 1288, 1164, 1118, 1098, 1071, 913, 779, 753, 737, 572 cm^{-1}. Selected X-ray crystallographic data: $P2_1/c$ (monoclinic), a = 17.7940(8) Å, b = 12.1974(5) Å, c = 18.4241(12) Å, β = 115.624(8)°, volume = 3605.5(4) Å^3, total reflections collected 18516, independent reflections 7327, R(int) = 0.035, R1 [$I > 2.0\sigma(I)$] = 0.0513, wR2 (all) = 0.1192, GOF = 0.997.

Preparation of $[(RNC)_2FePc]^+$ Complexes. Red $[(FcNC)_2FePc]^+$ and $[(t\text{-BuNC})_2FePc]^+$ complexes were prepared by reacting of 5−10 mg of the neutral compounds with 1.2 equiv of $[NO][BF_4]$ in 5 mL of dry DCM for 2 min. Subsequently, the reaction mixture was evaporated, and the red residue was washed several times with water and dried under vacuum. Data for $[(FcNC)_2FePc](BF_4)$ are as follows. UV−vis [DCM; λ, nm (log ε, M^{-1} cm^{-1})]: 822 (3.63), 719 (4.18), 514 (4.46), 419 (4.54), 301 (5.13). IR (KBr): 2165 [ν(CN)] cm^{-1}. Data for $[(t\text{-BuNC})_2FePc](BF_4)$ are as follows. UV−vis [DCM; λ, nm (log ε, M^{-1} cm^{-1})]: 813 (3.32), 713 (4.27), 519 (4.50), 420 (4.25), 306 (4.90). IR (KBr): 2177 [ν(CN)] cm^{-1}. Because of their highly reactive nature and limited thermal stability, repeated attempts to obtain satisfactory elemental analyses for $[(RNC)_2FePc]^+$ proved unsuccessful.

EPR samples of $[(RNC)_2FePc]^+$ (R = Fc, *t*-Bu) were prepared by oxidizing the corresponding neutral $(FcNC)_2FePc$ species with ca. 1.2 equiv of 2,3-dichloro-5,6-dicyano-1,4-benzoquinone (DDQ) in air-free DCM and transferring aliquots of the resulting solution into EPR tubes under argon.

Computational Details. All computations were performed using the *Gaussian 09* software package running under Windows or UNIX OS.[14] Molecular orbital (MO) contributions were compiled from single-point calculations using the *VMOdes* program.[15] In all single-point calculations, the B3LYP exchange-correlation functional[16] was used. The use of a pure generalized gradient approximation (BP86) exchange-correlation functional[17] led to an incorrect description of the highest occupied molecular orbital (HOMO) for $(FcNC)_2FePc$ and $(t\text{-BuNC})_2FePc$. Indeed, this later model predicted the HOMO of both complexes to be predominantly the d_{xy} orbital of the central metal atom, yet such a finding was not supported by the experimental electrochemical and spectroelectrochemical data. Wachter's full-electron basis set[18] was used for the iron atom(s), while the 6-31G(d) basis set[19] was employed for all other atoms during geometry optimization. A combination of Wachter's full-electron basis set for iron atom(s) and the 6-311G(d) basis set[20] for all other atoms was used for the single-point and TDDFT calculations. TDDFT calculations were conducted for the first 90 $[(FcNC)_2FePc]$ or 70 $[(t\text{-BuNC})_2FePc]$ excited states in order to ensure that all charge-transfer (CT) transitions of interest were calculated.

X-ray Crystallography. Slow crystallization of $(FcNC)_2FePc$ from a DCM/hexane system did not yield single crystals suitable for X-ray analysis. X-ray-quality single crystals of $(FcNC)_2FePc$ and $(t\text{-BuNC})_2FePc$ were grown by the slow diffusion of hexane into their saturated toluene solutions at room temperature. Experimental data for all compounds were collected using a Rigaku RAPID II X-ray diffractometer with curved IPDS detector employing graphite-monochromatized Mo Kα radiation (λ = 0.71075 Å).

The structures of the $(FcNC)_2FePc$ and $(t\text{-BuNC})_2FePc$ complexes were solved by direct methods using the *SIR-92* program.[21] All missed non-hydrogen atoms were located from analysis of a difference Fourier map and refined through isotropic and, subsequently, anisotropic approximations. All aromatic hydrogen atoms were placed in their

dx.doi.org/10.1021/ic4011423 | *Inorg. Chem.* 2013, 52, 11004−11012

geometrically expected positions, while the hydrogen atoms of the methyl groups were located from the difference Fourier map analysis. The isotropic thermal parameters of all hydrogen atoms were fixed to the values of the equivalent isotropic thermal parameters of the corresponding carbon atoms using riding model constraints so that $U_{iso}(H) = 1.2U_{eq}(C)$ for the non-methyl hydrogen atoms and $U_{iso}(H) = 1.5U_{eq}(C)$ for the methyl groups [$U_{eq} = {}^1/_3(U_{11} + U_{22} + U_{33})$]. Both structures were completely refined via the full-matrix least-squares method using the *Crystals for Windows* program.[22] Complete crystallographic information is available in the corresponding CIF in the Supporting Information (SI).

RESULTS AND DISCUSSION

Bis(isocyanoferrocene)iron(II) [$(FcNC)_2FePc$] was prepared by treating PcFe with excess FcNC in toluene followed by crystallization of the product from DCM/hexane. The "reference" compound, $(t\text{-BuNC})_2FePc$, was synthesized and isolated using a similar protocol (Scheme 1).

Scheme 1. Synthesis of the $(RNC)_2FePc$ Complexes

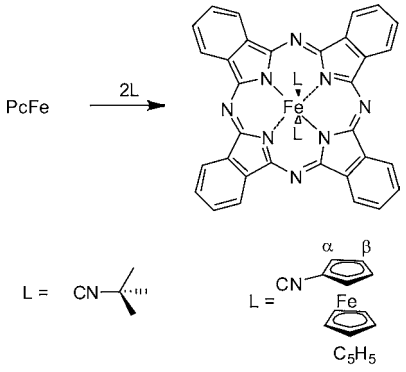

The molecular structures of $(FcNC)_2FePc$ and $(t\text{-BuNC})_2FePc$ were determined by X-ray crystallography (Figures 1 and SI 1−4 in the SI).[23] Although the DCM/hexane solvent system worked well for purification of the $(FcNC)_2FePc$ complex, it did not allow one to obtain X-ray-quality crystals of this compound. After exploring several other solvent combinations, we found that the slow evaporation of saturated solutions of $(FcNC)_2FePc$ in toluene/hexane afforded single crystals of this complex suitable for X-ray analysis. Not surprisingly, a toluene solvent molecule was found in the X-ray crystal structure of the $(FcNC)_2FePc$ complex. The CAMERON representations of the molecular structures of $(FcNC)_2FePc$ and $(t\text{-BuNC})_2FePc$ are shown in Figure 1, whereas selected bond distances and angles for these complexes are listed in Table 1.

Table 1. Selected Bond Distances (Å) and Angles (deg) for $(FcNC)_2FePc$ and $(t\text{-BuNC})_2FePc$ Complexes Determined by X-ray Crystallography

		$(t\text{-BuNC})_2FePc$	
	$(FcNC)_2FePc$	molecule 1	molecule 2
Fe−N(Pc)	1.944(3)	1.946(2)	1.947(3)
	1.952(3)	1.956(2)	1.951(3)
Fe−C	1.915(3)	1.929(3)	1.931(3)
C≡N	1.156(4)	1.156(4)	1.158(4)
≡N−C	1.397(4)	1.461(4)	1.469(4)
Fe−C(Fc, average)	2.041(4)		
N−Fe−N	89.64(11)	90.04(10)	89.57(11)
N−Fe−C≡	86.26(12)	84.64(11)	86.59(12)
	90.46(11)	89.54(11)	95.60(12)
Fe−C≡N	173.6(3)	169.1(3)	167.8(3)
C≡N−C	175.4(3)	166.5(3)	170.9(4)

Only half of the $(FcNC)_2FePc$ complex is crystallographically unique because its central iron(II) atom resides at a center of symmetry. Notably, the asymmetric unit of $(t\text{-BuNC})_2FePc$ contains the halves of two crystallographically independent molecules of the compound, with the central iron(II) atoms located at special crystallographic centers of symmetry. Both $(FcNC)_2FePc$ and $(t\text{-BuNC})_2FePc$ feature the central iron atom in a pseudooctahedral N4C2 environment, with the Fe−C bond distances being 0.02−0.03 Å shorter than the Fe−N bonds. The Fe−CN bond lengths in $(FcNC)_2FePc$ are statistically shorter than those in $(t\text{-BuNC})_2FePc$, reflecting a lower σ-donor/π-acceptor ratio[8] of the FcNC ligand compared to that of *t*-BuNC. The C≡N bond distances are within a typical range for isocyanide ligands coordinated to a transition-

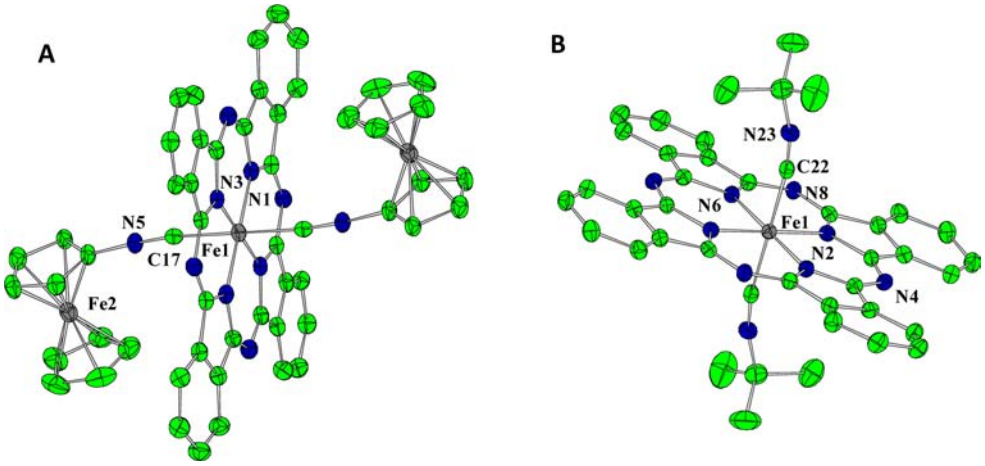

Figure 1. Molecular structures of $(FcNC)_2FePc$ (left) and $(t\text{-BuNC})_2FePc$ (right). 50% thermal ellipsoids. The toluene molecule of crystallization observed in the structure of $(FcNC)_2FePc$ is omitted for clarity. One of two crystallographically independent molecules of $(t\text{-BuNC})_2FePc$ in the asymmetric unit is shown. All hydrogen atoms are omitted for clarity.

dx.doi.org/10.1021/ic4011423 | *Inorg. Chem.* 2013, 52, 11004−11012

metal ion in an intermediate oxidation state.[8] The C−N−C and Fe−C−N angles are nearly linear, and the Pc cores are planar in both cases. The ferrocenyl groups in $(FcNC)_2FePc$ are locked in eclipsed conformations without significant disorder. All Fe−C(Fc) bond distances within the ferrocenyl substituents of $(FcNC)_2FePc$ are similar to those documented for other complexes of FcNC ligands.[8] Four ferrocenyl and four Pc moieties form a pocket in which two toluene molecules of crystallization are trapped (Figure SI 2 in the SI).

The well-known ring-current phenomenon[24] in FePc is responsible for substantial shielding (by 0.9−1.9 ppm) of the ^1H NMR resonances corresponding to the α-H, β-H, and C_5H_5 hydrogen nuclei of the ferrocenyl groups in $(FcNC)_2FePc$ compared to the free FcNC ligand.[25] Similarly, the ^1H resonance of the *t*-Bu substituents in $(t\text{-BuNC})_2FePc$ is shifted upfield with respect to free *t*-BuNC. In addition, in the IR spectra, the $\nu(C{\equiv}N)$ bands for $(FcNC)_2FePc$ and $(t\text{-BuNC})_2FePc$ complexes occur at ca. 10 cm^{-1} higher energy compared to the corresponding free RNC ligands[8,12] indicating a rather modest extent of backbonding interaction between the iron(II) center and the isocyanide ligands.

The UV−vis and MCD spectra of the $(FcNC)_2FePc$ and $(t\text{-BuNC})_2FePc$ complexes are virtually identical, as illustrated in Figure 2. Indeed, the UV−vis spectrum of $(FcNC)_2FePc$ consists of a Q band at 662 nm followed by two vibronic satellites at 634 and 599 nm. In addition, a low-intensity band is clearly observed at 394 nm, which is accompanied by a classic broad B band at 321 nm. On the other hand, the UV−vis spectrum of $(t\text{-BuNC})_2FePc$ features bands at 659, 635, 597, 395, and 322 nm, thereby indicating very similar energetics for the interactions involving the axial isocyanide ligands and the FePc core. In the MCD spectra of $(FcNC)_2FePc$, the Q and B bands are associated with the Faraday *A* terms centered at 661 and 319 nm, thus confirming the effective 4-fold local symmetry of the iron(II) phthalocyanine fragment. This is very typical for L_2FePc[26] and the other LMPc (M = Mg, Zn) complexes[27] that exhibit free rotation of the axial ligands around the Fe−L bond. Similarly, the Q and B bands in the MCD spectrum of $(t\text{-BuNC})_2FePc$ correspond to the Faraday *A* terms centered at 658 and 319 nm. The low-intensity band at 394 nm for $(FcNC)_2FePc$ or 395 nm for $(t\text{-BuNC})_2FePc$ is most likely associated with another *A* term, centered at the same energy; however, only its negative component located at 399 nm for $(FcNC)_2FePc$ or 400 nm for $(t\text{-BuNC})_2FePc$ is observed experimentally. The positive part of this *A* term is most likely obscured by other negative MCD signals of close energy, as has been documented earlier for $(NH_3)(CO)FePc$.[26] On the basis of the previous work by Stillman and co-workers[26,27] and one of us,[28] as well as the strong π-accepting capability of the axial isocyanide ligands, the above band can be preliminarily assigned as a metal-to-ligand charge-transfer [MLCT; Fe, $d_{xz,yz}$ → Pc, π^*] transition. While one might expect to observe additional Fc → Pc, π^* transitions in the UV−vis and MCD spectra of $(FcNC)_2FePc$, their presence is not obvious.

In order to explain the similarities of the UV−vis and MCD patterns documented for $(FcNC)_2FePc$ and $(t\text{-BuNC})_2FePc$ and gain additional insight into their electronic structures and redox behavior, we conducted DFT and TDDFT calculations on these complexes. MO diagrams for both compounds are presented in Figure 3, whereas MO compositions are summarized in Figure 4. In addition, selected MOs are depicted in Figure 3, while the full set of MOs is presented in the SI (Figure SI 5). The usual electronic configuration of a low-spin bisaxially coordinated iron(II) phthalocyanines is $(d_{xy})^2(d_{xz})^2(d_{yz})^2$. It may be expected that the strong π-acceptor character of the axial isocyanide ligands will lead to strong stabilization of the $d_{xz}d_{yz}$ MOs. Indeed, our DFT calculations predict that for both complexes the HOMO is a Pc-centered π MO. Thus, unlike in the case of classic L_2FePc complexes (L = nitrogen-based ligand),[29] the first oxidation of $(RNC)_2FePc$ should result in the formation of the corresponding Pc-centered cation radical, as was further confirmed by electrochemical, spectroelectrochemical, and EPR experiments

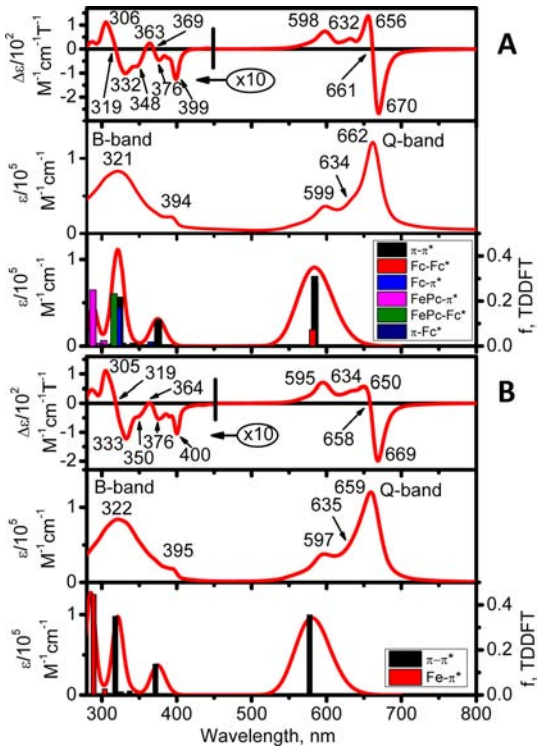

Figure 2. MCD (top) and experimental (middle) and TDDFT-predicted (bottom) UV−vis spectra of $(FcNC)_2FePc$ (A) and $(t\text{-BuNC})_2FePc$ (B).

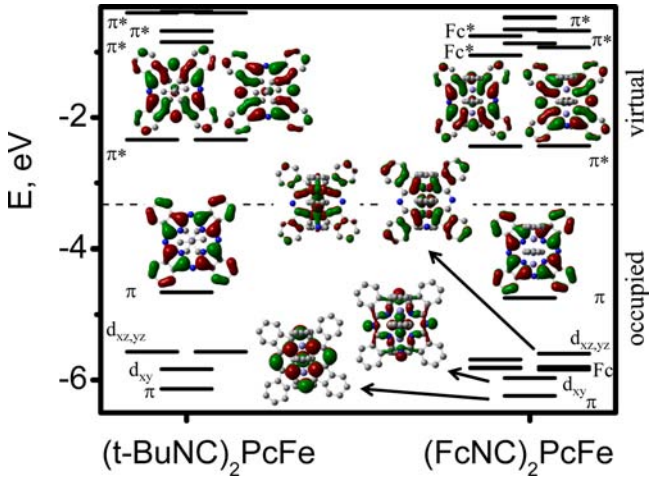

Figure 3. DFT-predicted orbital energy diagrams for $(t\text{-BuNC})_2FePc$ (left) and $(FcNC)_2FePc$ (right).

dx.doi.org/10.1021/ic4011423 | *Inorg. Chem.* 2013, 52, 11004−11012

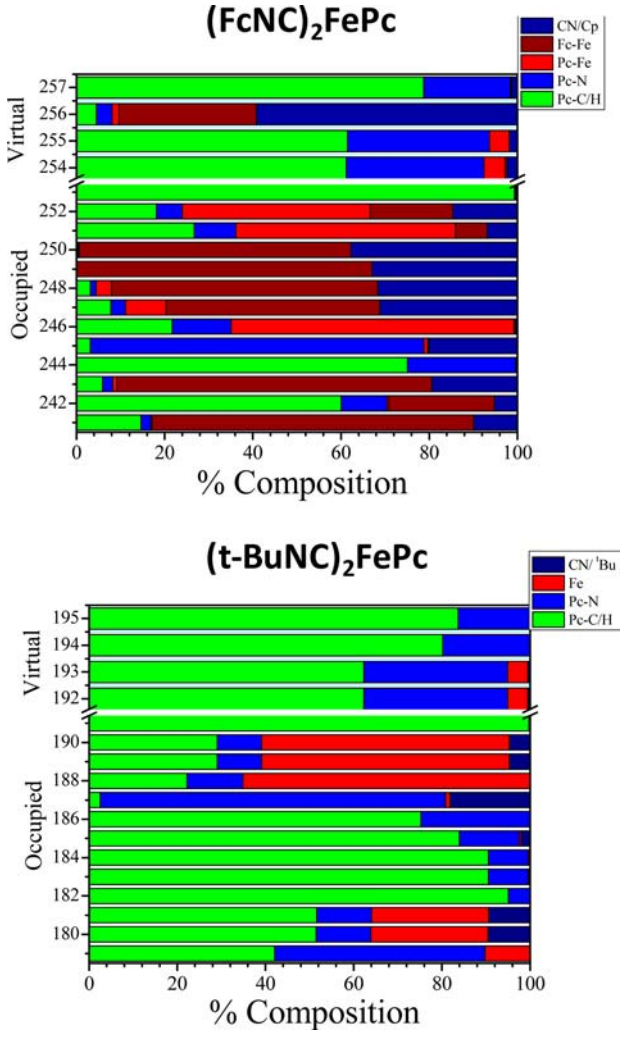

Figure 4. DFT-predicted MO composition diagrams for $(FcNC)_2FePc$ (top) and $(t\text{-}BuNC)_2FePc$ (bottom).

discussed below. Because of the strong-field nature of the axial isocyanide ligands, the iron(II) phthalocyanine's $d_{xz,yz}$ and d_{xy} orbitals are located between the Pc-centered a_{1u}-type HOMO and a_{2u}-type HOMO−4 [$(t\text{-}BuNC)_2FePc$] or HOMO−8 [$(FcNC)_2FePc$]. In addition, two sets of nearly degenerate ferrocenyl-centered MOs were predicted between the Pc-centered iron(II) $d_{xz,yz}$ and d_{xy} MOs in the case of the $(FcNC)_2FePc$ complex. The presence of these ferrocene-centered MOs between the a_{1u}-type HOMO and the a_{2u}-type HOMO−8 could potentially result in Fc → π^* (Pc) CT bands observable in the UV−vis spectrum of $(FcNC)_2FePc$ between the Pc-centered Q and B bands. Because of their delocalized nature, these MOs can also be potentially responsible for the weak metal−metal coupling documented for the $(FcNC)_2FePc$ complex. The nearly degenerate lowest unoccupied molecular orbital (LUMO) and LUMO+1 for both complexes are Pc-centered π^* MOs, and this is a usual situation for low-spin iron(II) phthalocyanines. Finally, several low-energy unoccupied MOs were predicted in the LUMO−LUMO+10 region (Figures 3, 4, and SI 5).

The TDDFT approach has proven to be instrumental for the accurate prediction of $\pi-\pi^*$ and CT energies and intensities in Pc's and their analogues.[30] The TDDFT-predicted electronic spectra of both $(RNC)_2FePc$ complexes are in excellent agreement with the corresponding experimental data (Figure 2) and are dominated by Pc-centered $\pi-\pi^*$ transitions. For both complexes, the Q-band region is dominated by HOMO → LUMO, LUMO+1 transitions typical for Pc complexes. The symmetry-forbidden A_g states, predominantly originating from the HOMO−1, HOMO−2 → LUMO, LUMO+1 [Fe($d_{xz,yz}$, Pc) → π^*(Pc)] transitions were predicted at ca. 520 and ca. 490 nm, while the allowed A_u symmetry states, proposed by Stillman et al.,[26] that originate from the Fe($d_{xz,yz}$, Pc) → π^*(Pc) transitions were predicted in the ca. 300 nm region. Both 395 nm and B-band regions are dominated by the Pc-centered $\pi-\pi^*$ transitions. In addition, in the case of the $(FcNC)_2FePc$ complex, two symmetry-forbidden A_g symmetry states and two symmetry-allowed A_u low-intensity symmetry states originating from the ferrocene-centered HOMO−3−HOMO−6 → LUMO+2−LUMO+8 transitions (Fc → Fc*) were predicted in the ca. 580 nm region. Because of the low intensity, these transitions, however, were not observed experimentally in the UV−vis and MCD spectra of $(FcNC)_2FePc$. Although the A_u states originating from the ferrocene-centered HOMO−3, HOMO−4 to Pc-centered LUMO, LUMO+1 transitions [Fc → π^*(Pc)] are symmetry-allowed, their intensities predicted by TDDFT are rather small, and thus such excited states cannot contribute significantly to the experimentally observed UV−vis and MCD spectra of $(FcNC)_2FePc$. Again, the TDDFT-predicted π(Pc) → Fc* transitions should have low intensities and provide only minor contributions to the predicted UV−vis and MCD patterns of $(FcNC)_2FePc$ in agreement with the experimental data. Overall, our TDDFT calculations suggest that the UV−vis and MCD spectra of the $(RNC)_2FePc$ complexes should be dominated by the Pc-centered $\pi-\pi^*$ transitions, thereby having very similar profiles, as indeed is observed experimentally.

The redox behavior of the $(RNC)_2FePc$ complexes described herein was addressed using electrochemical (CV and DPV; Figures 5 and SI 6 in the SI), spectroelectrochemical (Figures 6 and SI 7 in the SI), and chemical oxidation (Figures 7 and SI 8 in the SI) approaches. The reference complex $(t\text{-}BuNC)_2FePc$ was studied in DCM using two electrolyte systems: regular TBAP and noncoordinating TBAF. The former electrolyte was employed in order to compare our results with those obtained earlier by Hanack and co-workers for Pc-substituted (*t*-

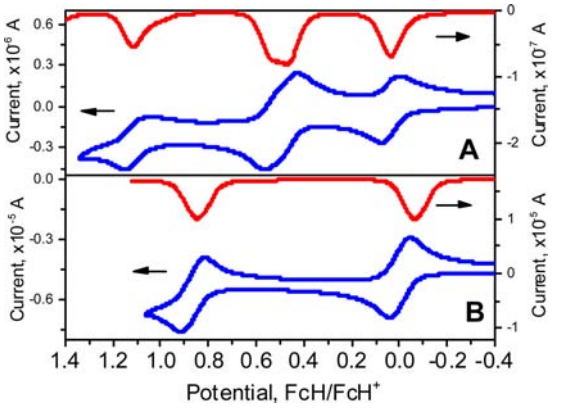

Figure 5. (A) DPV (red) and CV (blue) electrochemical data for $(FcNC)_2FePc$ ($E_{1/2}$, vs FcH/FcH^+ in DCM/0.05 M TBAF: +0.04, +0.47, +0.55, and +1.12 V). (B) DPV (red) and CV (blue) data for (*t*-$BuNC)_2FePc$ ($E_{1/2}$, vs FcH/FcH^+ in DCM/0.05 M TBAF: 0.00 and +0.86 V). In all cases, CV data were recorded at a rate of 100 mV/s.

dx.doi.org/10.1021/ic4011423 | *Inorg. Chem.* 2013, 52, 11004−11012

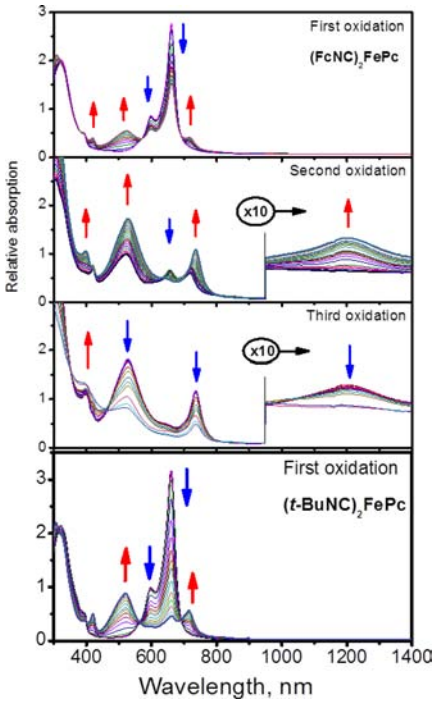

Figure 6. Spectroelectochemical oxidation of $(FcNC)_2FePc$ (top) and $(t\text{-BuNC})_2FePc$ (bottom) in a DCM/0.15 M TBAF system at room temperature.

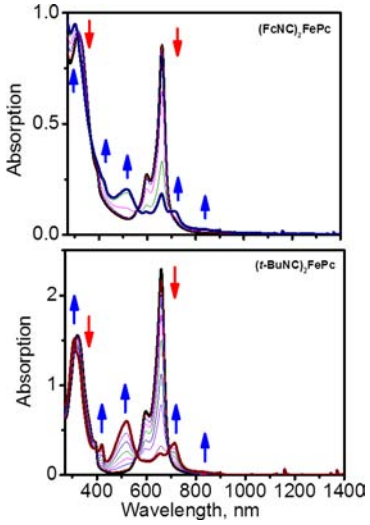

Figure 7. UV−vis spectra of the products of chemical oxidation of $(FcNC)_2FePc$ (top) and $(t\text{-BuNC})_2FePc$ (bottom) in DCM at room temperature using $[NO][BF_4]$ as an oxidant.

BuNC)$_2$FePc^R complexes,[31] while the later electrolyte was used to compare our electrochemical data acquired for (t-BuNC)$_2$FePc and $(FcNC)_2FePc$. The $(t\text{-BuNC})_2FePc$ complex dissolved in the traditional DCM/TBAP system shows one reversible and one irreversible oxidation waves in CV and DPV experiments, whereas both electrochemical processes for this compound in the DCM/TBAF solution appear to be reversible (Figure 5). The electrochemical data for $(FcNC)_2FePc$ were collected using a noncoordinating TBAF electrolyte because of its well-known advantages in investigating mixed-valence compounds.[32] The CV and DPV data for $(FcNC)_2FePc$ in a DCM/TBAF solution show that the complex exhibits four reversible oxidation waves, with the second and third waves being closely ($\Delta E_{1/2} \approx 80$ mV) spaced. The $E_{1/2}$ potentials for these second and third waves at +0.47 and +0.55 V, respectively, are comparable to that of the Fe^{II}/Fe^{III} couple (+0.42 V) reported for the oxidation of $[Cr(CNFc)_6]^{2+}$ under similar conditions.[12b]

The spectroelectrochemical and chemical oxidation data for the $(t\text{-BuNC})_2FePc$ complex correlate well with each other (Figures 6 and 7 and SI 8 in the SI). During the first oxidation process, the Q band at 659 nm disappears, the 395 nm band is reduced in intensity, and the B band shifts to 307 nm. In addition, three prominent new bands at 715, 520, and 420 nm appear in the UV−vis spectrum that are virtually independent of the nature of the oxidant. Similar spectroscopic changes have been observed for the numerous main-group and transition-metal Pc's under spectroelectrochemical and chemical oxidation conditions and indicate the formation of a classic red, Pc-centered cation radical.[33] While such oxidation of the Pc core in L_2FePc complexes is highly unusual,[29] this behavior has been previously documented for a series of closely related compounds.[9] The $[(t\text{-BuNC})_2FePc]^+$ species can also be generated by oxidizing the neutral $(t\text{-BuNC})_2FePc$ with 1 equiv of DDQ (Figure SI 8 in the SI). Its radical nature was confirmed by an EPR experiment, which indicates the presence of a cation radical delocalized over the Pc ligand with the EPR signature close to that of a free electron (Figure 8, top). Similar

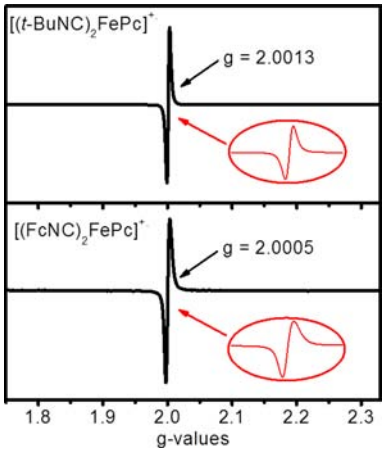

Figure 8. EPR spectra of $[(t\text{-BuNC})_2FePc]^+$ (top) and $[(FcNC)_2FePc]^+$ (bottom) in DCM at 77 K generated via oxidation of the corresponding neutral complexes with 1 equiv of DDQ.

EPR profiles had been previously observed in the case of main-group and transition-metal Pc cation radicals.[33] In addition, we isolated the red $[(t\text{-BuNC})_2FePc]^+$ complex via chemical oxidation of $(t\text{-BuNC})_2FePc$ with $[NO][BF_4]$ in DCM. The UV−vis spectrum of this product is in agreement with the corresponding spectroelectrochemical and chemical oxidation experiments (Figure SI 9 in the SI). The ν(CN) stretching band at 2177 cm^{-1} in the IR spectrum of $[(t\text{-BuNC})_2FePc]^+$ is significantly shifted compared to the same stretch observed for neutral $(t\text{-BuNC})_2FePc$ (2146 cm^{-1}). Notably, the cationic $[(t$-BuNC)$_2$FePc$]^+$ species can be quantitatively reduced to the initial neutral $(t\text{-BuNC})_2FePc$ complex under spectroelectrochemical conditions, which is in agreement with the reversibility of the first oxidation wave observed in our electrochemical experiments. Such reversibility also rules out the possibility of an axial ligand dissociation in this complex

dx.doi.org/10.1021/ic4011423 | Inorg. Chem. 2013, 52, 11004−11012

during the first oxidation process. The subsequent oxidation of $[(t\text{-BuNC})_2FePc]^+$ under chemical and spectroelectrochemical conditions results in partial or complete degradation of the compound. Indeed, in our spectroelectrochemical experiment in the DCM/TBAF system, about one-third of the complex was found to deteriorate based on assessment of the reduction data, and thus spectroscopic data for the $[(t\text{-BuNC})_2FePc]^{2+}$ complex cannot be considered reliable, at least from a quantitative standpoint.

The first oxidation process observed for $(FcNC)_2FePc$ is similar to that observed for $(t\text{-BuNC})_2FePc$ and results in the formation of a red, Pc-centered cation radical. Again, upon either spectroelectrochemical or chemical oxidation of the neutral species, the original Q band disappears, while the B band shifts to 309 nm (Figures 6 and 7 and SI 8 in the SI). In addition, three new intense bands at 716, 524, and 420 nm appear in the UV−vis spectrum. The UV−vis spectrum of the isolated $[(FcNC)_2FePc]^+$ complex is similar to that obtained under spectroelectrochemical and chemical oxidation conditions. The EPR spectrum of the $[(FcNC)_2FePc]^+$ cation radical in DCM at 77 K, which was generated via oxidation of its neutral precursor with DDQ, is reminiscent of that of a free electron (Figure 8, bottom), thereby indicating the formation of a classic Pc-centered cation radical.[9,33] It should be noted, however, that the EPR signal of this complex is significantly broader compared to that observed for $[(t\text{-BuNC})_2FePc]^+$, which may suggest a higher degree of spin delocalization in the $[(FcNC)_2FePc]^+$ system. This EPR signal disappears completely in the 150−175 K temperature range. Similar to what was observed for the $[(t\text{-BuNC})_2FePc]^{0/+}$pair, the ν(CN) stretching band at 2165 cm^{-1} in the IR spectrum of $[(FcNC)_2FePc]^+$ is significantly shifted compared to that at 2132 cm^{-1} for neutral $(FcNC)_2FePc$.

Further oxidation of the $[(FcNC)_2FePc]^+$ complex under spectroelectrochemical conditions leads to generation of the mixed-valence dication $[(FcNC)_2FePc]^{2+}$, which exhibits a characteristic low-energy intervalence charge-transfer (IVCT) band at about 1200 nm (Figure 6). This IVCT band disappears upon transformation of $[(FcNC)_2FePc]^{2+}$ into $[(FcNC)_2FePc]^{3+}$, which could be easily reduced to the neutral $(FcNC)_2FePc$ species without loss of the Q-band intensity (Figure SI 7 in the SI). Although the 80 mV separation between the waves corresponding to the sequential oxidation of the first and second ferrocenyl moieties (K_c = 24.3; see, however, a cautionary warning on the use of K_c values obtained from the electrochemical data for analysis of mixed-valence compounds)[34] is significantly smaller compared to those documented for a number of previously studied organometallic porphyrins,[7] it is still indicative of electronic communication between the two FcNC ligands in $(FcNC)_2FePc$ in which the iron centers are separated by ca. 11.5 Å. Analysis of the IVCT band[35] allows estimation of the H_{ab} (335 cm^{-1}) and α^2 (1.6×10^{-3}) parameters for the mixed-valence $[(FcNC)_2FePc]^{2+}$ species, which can be viewed as a class II (Robin−Day classification)[36] weakly coupled system. Our attempts to isolate the mixed-valence $[(FcNC)_2FePc]^{2+}$ complex by chemical oxidation invariably failed probably because of its rather poor thermal stability and the small difference between the second and third oxidation potentials of $(FcNC)_2FePc$.

CONCLUDING REMARKS

Herein, we describe the synthesis, structure, redox behavior, and extensive spectroscopic characterization of an unusual iron(II) phthalocyanine complex axially coordinated with redox-active isocyanide ligands. The chemical or electrochemical oxidation of $(RNC)_2FePc$ (R = *t*-Bu or Fc) affords the corresponding Pc-centered $[(RNC)_2FePc]^+$ cation radicals. The radical nature of these species was corroborated by UV−vis and EPR spectroscopic methods. Despite a relatively large distance (11.5 Å) between the two iron centers of the FcNC ligands in $(FcNC)_2FePc$, we documented weak electronic communication between them and observed an IVCT band for the mixed-valence $[(FcNC)_2FePc]^{2+}$ complex in the near-IR region, which is suggestive of class II behavior (under Robin−Day classification) of mixed valency.

ASSOCIATED CONTENT

Supporting Information

X-ray crystallographic data in CIF format and spectroscopic, crystallographic, and DFT data for $(FcNC)_2FePc$ and $(t\text{-BuNC})_2FePc$. This material is available free of charge via the Internet at http://pubs.acs.org.

AUTHOR INFORMATION

Corresponding Authors

*E-mail: vnemykin@d.umn.edu.
*E-mail: mbarybin@ku.edu.

Notes

The authors declare no competing financial interest.

ACKNOWLEDGMENTS

Generous support by NSF Grant CHE-1110455 and NSF MRI Grant CHE-0922366, Minnesota Supercomputing Institute, and University of Minnesota Grant-in-Aid to V.N.N., as well as NSF Grant CHE-1214102 to M.V.B., is greatly appreciated. The authors acknowledge NSF CRIF Grant CHE-0946883 for funds to purchase the EPR instrument.

REFERENCES

(1) (a) Muraoka, T.; Kinbara, K.; Aida, T. *Nature* **2006**, *440*, 512. (b) Bucher, C.; Bayley, C. H. *Nature* **2010**, *467*, 164. (c) Jurow, M.; Schuckman, A. E.; Batteas, J. D.; Drain, C. M. *Coord. Chem. Rev.* **2010**, *254*, 2297. (d) Barybin, M. V. *Coord. Chem. Rev.* **2010**, *254*, 1240.

(2) (a) Nemykin, V. N.; Kobayashi, N. *Chem. Commun.* **2001**, 165. (b) Lukyanets, E. A.; Nemykin, V. N. *J. Porphyrins Phthalocyanines* **2010**, *14*, 1.

(3) (a) Jin, Z.; Nolan, K.; McArthur, C. R.; Lever, A. B. P.; Leznoff, C. C. *J. Organomet. Chem.* **1994**, *468*, 205. (b) Poon, K.-W.; Yan, Y.; Li, X. Y.; Ng, D. K. P. *Organometallics* **1999**, *18*, 3528. (c) Nemykin, V. N.; Lukyanets, E. A. *ARKIVOC* **2010**, *(i)*, 136. (d) An, M.; Kim, S.; Hong, J.-D. *Bull. Korean Chem. Soc.* **2010**, *31*, 3272. (e) Gonzalez-Cabello, A.; Claessens, C. G.; Martin-Fuch, G.; Ledoux-Rack, I.; Vazquez, P.; Zyss, J.; Agullo-Lopez, F.; Torres, T. *Synth. Met.* **2003**, *137*, 1487. (f) Gonzalez-Cabello, A.; Vazquez, P.; Torres, T. *J. Organomet. Chem.* **2001**, *637*−*639*, 751.

(4) (a) Gryko, D. T.; Piechowska, J.; Jaworski, J. S.; Galezowski, M.; Tasior, M.; Cembor, M.; Butenschoen, H. *New J. Chem.* **2007**, *31*, 1613. (b) Venkatraman, S.; Kumar, R.; Sankar, J.; Chandrashekar, T. K.; Sendhil, K.; Vijayan, C.; Kelling, A.; Senge, M. O. *Chem.—Eur. J.* **2004**, *10*, 1423. (c) Kumar, R.; Misra, R.; Prabhu-Raja, V.; Chandrashekar, T. K. *Chem.—Eur. J.* **2005**, *11*, 5695.

(5) (a) Devillers, H.; Moutet, J.-C.; Royal, G.; Saint-Aman, E. *Coord. Chem. Rev.* **2009**, *253*, 21. (b) Suijkerbuijk, B. M. J. M.; Gebbink, R. J. M. K. *Angew. Chem., Int. Ed.* **2008**, *47*, 7396. (c) Vecchi, A.; Galloni, P.; Floris, B.; Nemykin, V. N. *J. Porphyrins Phthalocyanines* **2013**, *17*, 165. (d) Rohde, G. T.; Sabin, J. R.; Barrett, C. D.; Nemykin, V. N. *New J. Chem.* **2011**, *35*, 1440. (e) Nemykin, V. N.; Galloni, P.; Floris, B.; Barrett, C. D.; Hadt, R. G.; Subbotin, R. I.; Marrani, A. G.; Zanoni, R.;

Loim, N. M. *Dalton Trans.* **2008**, 4233. (f) Nemykin, V. N.; Barrett, C. D.; Hadt, R. G.; Subbotin, R. I.; Maximov, A. Y.; Polshin, E. V.; Koposov, A. Y. *Dalton Trans.* **2007**, 3378. (g) Loim, N. M.; Abramova, N. V.; Sokolov, V. I. *Mendeleev Commun.* **1996**, 46. (h) Burrell, A. K.; Campbell, W. M.; Jameson, G. B.; Officer, D. L.; Boyd, P. D. W.; Zhao, Z.; Cocks, P. A.; Gordon, K. C. *Chem. Commun.* **1999**, 637. (i) Narayanan, S. J.; Venkatraman, S.; Dey, S. R.; Sridevi, B.; Anand, V. R. G.; Chandrashekar, T. K. *Synlett* **2000**, 1834. (j) Rhee, S. W.; Na, Y. H.; Do, Y.; Kim, J. *Inorg. Chim. Acta* **2000**, *309*, 49. (k) Shoji, O.; Okada, S.; Satake, A.; Kobuke, Y. *J. Am. Chem. Soc.* **2005**, *127*, 2201. (l) Shoji, O.; Tanaka, H.; Kawai, T.; Kobuke, Y. *J. Am. Chem. Soc.* **2005**, *127*, 8598. (m) Auger, A.; Swarts, J. C. *Organometallics* **2007**, *26*, 102. (n) Kubo, M.; Mori, Y.; Otani, M.; Murakami, M.; Ishibashi, Y.; Yasuda, M.; Hosomizu, K.; Miyasaka, H.; Imahori, H.; Nakashima, S. *J. Phys. Chem. A* **2007**, *111*, 5136.

(6) (a) Shoji, O.; Okada, S.; Satake, A.; Kobuke, Y. *J. Am. Chem. Soc.* **2005**, *127*, 2201. (b) Rochford, J.; Rooney, A. D.; Pryce, M. T. *Inorg. Chem.* **2007**, *46*, 7247. (c) Nemykin, V. N.; Rohde, G. T.; Barrett, C. D.; Hadt, R. G.; Bizzarri, C.; Galloni, P.; Floris, B.; Nowik, I.; Herber, R. H.; Marrani, A. G.; Zanoni, R.; Loim, N. M. *J. Am. Chem. Soc.* **2009**, *131*, 14969. (d) Nemykin, V. N.; Rohde, G. T.; Barrett, C. D.; Hadt, R. G.; Sabin, J. R.; Reina, G.; Galloni, P.; Floris, B. *Inorg. Chem.* **2010**, *49*, 7497. (e) Galloni, P.; Floris, B.; de Cola, L.; Cecchetto, E.; Williams, R. M. *J. Phys. Chem. C* **2007**, *111*, 1517. (f) Solntsev, P. V.; Neisen, B. D.; Sabin, J. R.; Gerasimchuk, N. N.; Nemykin, V. N. *J. Porphyrins Phthalocyanines* **2011**, *15*, 612. (g) Vecchi, A.; Gatto, E.; Floris, B.; Conte, V.; Venanzi, M.; Nemykin, V. N.; Galloni, P. *Chem. Commun.* **2012**, *48*, 5145. (h) Solntsev, P. V.; Spurgin, K. L.; Sabin, J. R.; Heikal, A. A.; Nemykin, V. N. *Inorg. Chem.* **2012**, *51*, 6537.

(7) (a) Maiya, G. B.; Barbe, J. M.; Kadish, K. M. *Inorg. Chem.* **1989**, *28*, 2524. (b) Solntsev, P. V.; Sabin, J. R.; Dammer, S. J.; Gerasimchuk, N. N.; Nemykin, V. N. *Chem. Commun.* **2010**, *46*, 6581. (c) Xu, Q. Y.; Barbe, J. M.; Kadish, K. M. *Inorg. Chem.* **1988**, *27*, 2373.

(8) Barybin, M. V.; Meyers, J. J., Jr.; Neal, B. M. Renaissance of Isocyanoarenes as Ligands in Low-Valent Organometallics. In *Isocyanide Chemistry—Applications in Synthesis and Material Science*; Nenajdenko, V., Ed.; Wiley-VCH: Weinheim, Germany, 2012; pp 493−529.

(9) (a) Hanack, M.; Kamenzin, S.; Kamenzin, C.; Subramanian, L. R. *Synth. Met.* **2000**, *110*, 93. (b) Hanack, M.; Hees, M.; Witke, E. *New J. Chem.* **1998**, *22*, 169. (c) Watkins, J. J.; Balch, A. L. *Inorg. Chem.* **1975**, *14*, 2720.

(10) Ryu, H.; Knecht, S.; Subramanian, L. R.; Hanack, M. *Synth. Met.* **1995**, *72*, 289.

(11) (a) Barriere, F.; Geiger, W. E. *J. Am. Chem. Soc.* **2006**, *128*, 3980. (b) Geiger, W. E.; Connelly, N. G. *Adv. Organomet. Chem.* **1985**, *24*, 87.

(12) (a) Barybin, M. V.; Holovics, T. C.; Deplazes, S. F.; Lushington, G. H.; Powell, D. R.; Toriyama, M. *J. Am. Chem. Soc.* **2002**, *124*, 13668. (b) Holovics, T. C.; Deplazes, S. F.; Toriyama, M.; Powell, D. R.; Lushington, G. H.; Barybin, M. V. *Organometallics* **2004**, *23*, 2927.

(13) Hanack, M.; Ryu, H. *Synth. Met.* **1992**, *46*, 113.

(14) Frisch, M. J.; Trucks, G. W.; Schlegel, H. B.; Scuseria, G. E.; Robb, M. A.; Cheeseman, J. R.; Montgomery, J. A., Jr.; Vreven, T.; et al. *Gaussian 09*, revision A.01; Gaussian, Inc.: Wallingford, CT, 2009. See the SI for full citation.

(15) Nemykin,V. N.; Basu, P. *VMOdes Program*, revision A7.2; University of Minnesota—Duluth and Duquesne University: Duluth, MN, and Pittsburgh, PA, 2005.

(16) (a) Becke, A. D. *J. Chem. Phys.* **1993**, *98*, 5648. (b) Lee, C.; Yang, W.; Parr, R. G. *Phys. Rev. B* **1988**, *37*, 785.

(17) (a) Becke, A. D. *Phys. Rev. A* **1988**, *38*, 3098. (b) Perdew, J. P. *Phys. Rev. B* **1986**, *33*, 8822.

(18) Wachters, A. J. H. *J. Chem. Phys.* **1970**, *52*, 1033.

(19) (a) Hehre, W. J.; Ditchfield, R.; Pople, J. A. *J. Chem. Phys.* **1972**, *56*, 2257. (b) Gordon, M. S. *Chem. Phys. Lett.* **1980**, *76*, 163.

(20) McLean, A. D.; Chandler, G. S. *J. Chem. Phys.* **1980**, *72*, 5639.

(21) Altomare, A.; Cascarano, G.; Giacovazzo, C.; Guagliardi, A.; Burla, M. C.; Polidori, G.; Camalli, M. *J. Appl. Crystallogr.* **1994**, *27*, 435.

(22) Betteridge, P. W.; Carruthers, J. R.; Cooper, R. I.; Prout, K.; Watkin, D. J. *J. Appl. Crystallogr.* **2003**, *36*, 1487.

(23) During the preparation of this manuscript, we became aware that a similar structure for $(t\text{-BuNC})_2$FePc has been reported: Janczak, J.; Kubiak, R.; Lisowski, J. *J. Porphyrins Phthalocyanines* **2013**, *17*, in press, DOI: 10.1142/S1088424613500181.

(24) (a) Choy, C. K.; Mooney, J. R.; Kenney, M. E. *J. Magn. Reson.* **1979**, *35*, 1. (b) Nemykin, V. N.; Kobayashi, N.; Chernii, V. Y.; Belsky, V. K. *Eur. J. Inorg. Chem.* **2001**, 733. (c) Ona-Burgos, P.; Casimiro, M.; Fernandez, I.; Navarro, A. V.; Fernandez Sanchez, J. F.; Carretero, A. S.; Gutierrez, A. F. *Dalton Trans.* **2010**, *39*, 6231. (d) Nemykin, V. N.; Chernii, V. Ya.; Volkov, S. V.; Bundina, N. I.; Kaliya, O. L.; Li, V. D.; Lukyanets, E. A. *J. Porphyrins Phthalocyanines* **1999**, *3*, 87.

(25) Holovics, T. C.; Deplazes, S. F.; Toriyama, M.; Powell, D. R.; Lushington, G. H.; Barybin, M. V. *Organometallics* **2004**, *23*, 2927.

(26) Ough, E. A.; Stillman, M. J. *Inorg. Chem.* **1994**, *33*, 573.

(27) (a) Sabin, J. R.; Varzatskii, O. A.; Voloshin, Y. Z.; Starikova, Z. A.; Novikov, V. V.; Nemykin, V. N. *Inorg. Chem.* **2012**, *51*, 8362. (b) Ishii, K.; Hirose, Y.; Kobayashi, N. *J. Porphyrins Phthalocyanines* **1999**, *3*, 6. (c) Mack, J.; Stillman, M. J. *J. Phys. Chem.* **1995**, *99*, 7935. (d) Kobayashi, N.; Nakajima, S.; Ogata, H.; Fukuda, T. *Chem.—Eur. J.* **2004**, *10*, 6294.

(28) Nemykin, V. N.; Polshina, A. E.; Chernii, V. Y.; Polshin, E. V.; Kobayashi, N. *Dalton Trans.* **2000**, 1019.

(29) (a) L'Her, M.; Pondaven, A. In *Porphyrin Handbook*; Kadish, K. M., Smith, K. M., Guilard, R., Eds.; Academic Press: New York, 2003; Vol. *16*, pp 117−169. (b) Kadish, K. M.; Bottomley, L. A.; Cheng, J. S. *J. Am. Chem. Soc.* **1978**, *100*, 2731. (c) Lever, A. B. P.; Wilshire, J. P. *Inorg. Chem.* **1978**, *17*, 1145.

(30) (a) Nemykin, V. N.; Hadt, R. G. *J. Phys. Chem. A* **2010**, *114*, 12062. (b) Nemykin, V. N.; Hadt, R. G.; Belosludov, R. V.; Mizuseki, H.; Kawazoe, Y. *J. Phys. Chem. A* **2007**, *111*, 12901. (c) Zhang, L.; Qi, D.; Zhang, Y.; Bian, Y.; Jiang, J. *J. Mol. Graphics Modell.* **2011**, *29*, 717. (d) Zarate, X.; Schott, E.; Arratia-Perez, R. *Int. J. Quantum Chem.* **2011**, *111*, 4186. (e) Soldatova, A. V.; Kim, J.-H.; Rizzoli, C.; Kenney, M. E.; Rodgers, M. A. J.; Rosa, A.; Ricciardi, G. *Inorg. Chem.* **2011**, *50*, 1135. (f) Ricciardi, G.; Soldatova, A. V.; Rosa, A. *J. Porphyrins Phthalocyanines* **2010**, *14*, 689. (g) Gao, Y.; Nemykin, V. N. *J. Mol. Graphics Modell.* **2013**, *42*, 73. (h) Gao, Y.; Solntsev, P. V.; Nemykin, V. N. *J. Mol. Graphics Modell.* **2012**, *38*, 369. (i) Nemykin, V. N.; Sabin, J. R. *J. Phys. Chem. A* **2012**, *116*, 7364. (j) Li, Y. L.; Han, L.; Mei, Y.; Zhang, J. Z. H. *Chem. Phys. Lett.* **2009**, *482*, 217−222. (k) Fabrizi de Biani, F.; Manca, G.; Marchetti, L.; Leoni, P.; Bruzzone, S.; Guidotti, C.; Atrei, A.; Albinati, A.; Rizzato, S. *Inorg. Chem.* **2009**, *48*, 10126−10137. (l) Li, F.; Sa, R.; Wu, K. *Mol. Phys.* **2008**, *106*, 2537−2544. (m) Peralta, G. A.; Seth, M.; Zhekova, H.; Ziegler, T. *Inorg. Chem.* **2008**, *47*, 4185. (n) Peralta, G. A.; Seth, M.; Ziegler, T. *Inorg. Chem.* **2007**, *46*, 9111. (o) Mack, J.; Sosa-Vargas, L.; Coles, S. J.; Tizzard, G. J.; Chambrier, I.; Cammidge, A. N.; Cook, M. J.; Kobayashi, N. *Inorg. Chem.* **2012**, *51*, 12820. (p) Mack, J.; Kobayashi, N.; Stillman, M. J. *J. Inorg. Biochem.* **2010**, *104*, 310. (q) Sumimoto, M.; Kawashima, Y.; Yokogawa, D.; Hori, K.; Fujumoto, H. *Int. J. Quantum Chem.* **2013**, *113*, 272.

(31) Schmid, G.; Witke, E.; Schlick, U.; Knecht, S.; Hanack, M. *J. Mater. Chem.* **1995**, *5*, 855.

(32) (a) Solntsev, P. V.; Dudkin, S. V.; Sabin, J. R.; Nemykin, V. N. *Organometallics* **2011**, *30*, 3037. (b) Hildebrandt, A.; Lehrich, S. W.; Schaarschmidt, D.; Jaeschke, R.; Schreiter, K.; Spange, S.; Lang, H. *Eur. J. Inorg. Chem.* **2012**, *2012*, 1114. (c) Hildebrandt, A.; Schaarschmidt, D.; Claus, R.; Lang, H. *Inorg. Chem.* **2011**, *50*, 10623. (d) Hildebrandt, A.; Schaarschmidt, D.; Lang, H. *Organometallics* **2011**, *30*, 556.

(33) (a) Ferraudi, G.; Oishi, S.; Muraldiharan, S. *J. Phys. Chem.* **1984**, *88*, 5261. (b) Nyokong, T.; Gasyna, Z.; Stillman, M. J. *Inorg. Chim. Acta* **1986**, *112*, 11. (c) Gavrilov, V. I.; Konstantinov, A. P.; Derkacheva, V. M.; Lukyanets, E. A.; Shelepin, I. V. *Zh. Fiz. Khim.* **1986**, *60*, 1448. (d) Nyokong, T.; Gasyna, Z.; Stillman, M. J. *Inorg.*

Chem. **1987**, *26*, 548. (e) Nyokong, T.; Gasyna, Z.; Stillman, M. J. *Inorg. Chem.* **1987**, *26*, 1087. (f) Ough, E.; Gasyna, Z.; Stillman, M. J. *Inorg. Chem.* **1991**, *30*, 2301. (g) Ostendorp, G.; Sieverdorp, G.; Homborg, H. *Z. Anorg. Allg. Chem.* **1995**, *621*, 451. (h) Gebauer, A.; Dawson, D. Y.; Arnold, J. *J. Chem. Soc., Dalton Trans.* **2000**, 111.

(34) (a) D'Alessandro, D. M.; Keene, F. R. *Dalton Trans.* **2004**, 3950. (b) D'Alessandro, D.; Keene, R. *Chem. Soc. Rev.* **2006**, *35*, 424.

(35) (a) Hush, N. S. *Prog. Inorg. Chem.* **1967**, *8*, 391. (b) Creutz, C. *Prog. Inorg. Chem.* **1983**, *30*, 1−73. (c) Hush, N. S. *Coord. Chem. Rev.* **1985**, *64*, 135.

(36) Robin, M. B.; Day, P. *Adv. Inorg. Chem. Radiochem.* **1967**, *10*, 247.